

A Unified Framework for Joint Registration and Segmentation

Konstantin Ens^{a,b}, Jens von Berg^b, Sven Kabus^b, Cristian Lorenz^b, and Bernd Fischer^a

^aInstitute of Mathematics, University of Lübeck, Wallstrasse 40, 23560 Lübeck, Germany;

^bPhilips Research Europe – Hamburg, Röntgenstrasse 24-26, 22335 Hamburg, Germany.

ABSTRACT

Accurate image registration is a necessary prerequisite for many diagnostic and therapy planning procedures where complementary information from different images has to be combined. The design of robust and reliable non-parametric registration schemes is currently a very active research area. Modern approaches combine the pure registration scheme with other image processing routines such that both ingredients may benefit from each other. One of the new approaches is the combination of segmentation and registration (segristration). Here, the segmentation part guides the registration to its wanted configuration, whereas on the other hand the registration does lead to an automatic segmentation. By joining these image processing methods it is possible to overcome some of the pitfalls of the individual methods. Here, we focus on the benefits of the registration part.

In¹ we presented a framework for non-parametric image registration improved through manual segmentation (weighted image registration). We demonstrated that this technique considerably improves registration results. A next step is the investigation of automatic segmentation schemes. In the current work, we present a novel unified framework for non-parametric registration combined with segmentation through active contours. In the literature, one may find various ways to combine these image processing routines. Here, we present the most promising approaches within the general framework. It is based on a variational formulation of both the registration and the segmentation part. The performance tests are carried out for magnet resonance brain images, which demonstrate the potential of the proposed methods.

Keywords: segristration, medical image registration, segmentation, mathematical modeling, brain images, magnet resonance imaging

1. INTRODUCTION

Medical image registration is still one of today's most challenging imaging problems.²⁻⁵ Here, we consider the use of non-parametric and non-linear registration schemes. Their intrinsic flexibility allows for the incorporation of extern regularization and thereby for the design of application adapted registration schemes. One way of introducing an extern regularization into the scheme is the use of a segmentation term within the energy functional of registration. The goal is to improve the results of registration for a region of interest. For example, in magnet resonance brain images one may in particular be interested in white matter, gray matter, or cerebrospinal fluid regions.

In this paper we design and discuss a promising unified framework for joint non-parametric image registration combined with segmentation through active contours. This framework allows one to unify existing registration / segmentation schemes, to easily design new ones, and to compare and validate the various in the literature described methods in a systematic fashion.

In the following we set up the notation for non-parametric image registration and energy-based segmentation.

1.1. Non-parametric image registration

We start out by defining the non-parametric image registration problem in a variational setting. Given a reference image \mathbf{R} and a template image \mathbf{T} , to be transformed, where $\mathbf{R}, \mathbf{T} : \Omega \rightarrow]0, 1[^d \rightarrow \mathbb{R}$. We wish to find a displacement field \mathbf{Y} that minimizes the following functional

Further author information: (Send correspondence to K.E.)

K.E.: E-mail: Ens (at) math.uni-luebeck.de

$$J_{REG}(\mathbf{Y}; \mathbf{R}, \mathbf{T}) = \alpha_1 \cdot S(\mathbf{Y}) + D(\mathbf{Y}; \mathbf{R}, \mathbf{T}). \quad (1)$$

Here, S denotes a regularizer for the displacement field \mathbf{Y} . The specific choice of the regularizer is not in the focus of this work (for an overview, we refer to⁶). For the examples to be presented, we have used the so-called elastic potential⁷

$$S(\mathbf{Y}) = \int_{\Omega} \frac{\mu}{4} \sum_{j,k=1}^d (\partial_j Y_k(\mathbf{x}) + \partial_k Y_j(\mathbf{x}))^2 + \frac{\lambda}{2} (\operatorname{div} \mathbf{Y}(\mathbf{x}))^2 d\mathbf{x} \quad (2)$$

where μ and λ are so-called Lamé-constants describing the elasticity of the underlying material. D is a distance measure quantifying the similarity between the reference image \mathbf{R} and the deformed template image $\mathbf{T}_{\mathbf{Y}}(\mathbf{x}) = \mathbf{T}(\mathbf{Y}(\mathbf{x}))$. We have chosen the mutual information (MI)⁸ for our experiments, a well known concept from information theory and a standard distance measure in multi-modal image registration. More precisely

$$D(\mathbf{Y}; \mathbf{R}, \mathbf{T}) = - \int_{\mathbb{R}} \int_{\mathbb{R}} \mathbf{p}_{\mathbf{R}\mathbf{T}_{\mathbf{Y}}}(r, t) \log \left(\frac{\mathbf{p}_{\mathbf{R}\mathbf{T}_{\mathbf{Y}}}(r, t)}{\mathbf{p}_{\mathbf{R}}(r) \mathbf{p}_{\mathbf{T}_{\mathbf{Y}}}(t)} \right) dr dt, \quad (3)$$

where $\mathbf{p}_{\mathbf{R}}(\cdot)$, $\mathbf{p}_{\mathbf{T}_{\mathbf{Y}}}(\cdot)$ are marginal probability distributions of the gray values in the images \mathbf{R} and $\mathbf{T}_{\mathbf{Y}}$ and $\mathbf{p}_{\mathbf{R}\mathbf{T}_{\mathbf{Y}}}(\cdot, \cdot)$ stands for the joint gray-value probability distribution of both images.

The regularization parameter α_1 controls the impact of the ingredients. The parameters α_2, β_i , to be introduced later, have a similar role.

1.2. Energy-based segmentation

Next, we present a variational formulation for the segmentation problem. The objective is to minimize the energy functional

$$J_{SEG}(\mathbf{C}; \mathbf{I}) = \alpha_2 \cdot E_{\text{ext}}(\mathbf{C}; \mathbf{I}) + E_{\text{int}}(\mathbf{C}) \quad (4)$$

with respect to the set \mathbf{C} , containing a finite set of smooth, closed curves $C: [0, 1] \rightarrow \Omega \subset \mathbb{R}^d$, which eventually define the segmentation. The particular representation of the curve is not in the focus of this work (for an overview we refer to⁹). For the examples to be presented, we have employed the widely used implicit representations via Level Sets.^{10, 11} Furthermore, \mathbf{I} denotes the image under consideration. E_{int} acts solely on the curve and is therefore frequently called internal energy. It controls the smoothness of the curve. Typical smoothers are based on the length or on the area enclosed by the curve. Here, we use the length of the curve. E_{ext} should drive the curve to its destination and is known as external energy. For our experiments we use a variation of the Mumford-Shah functional¹² introduced by Chan and Vese.^{13, ?} Their so-called multiphase energy functional is based on two sets of curves $\mathbf{C}_1, \mathbf{C}_2$ and reads as follows

$$E_{\text{ext}}(\mathbf{C}_1, \mathbf{C}_2; \mathbf{I}) = \int_{\mathbf{I}_{11}} |\mathbf{I} - c_{11}|^2 dx + \int_{\mathbf{I}_{10}} |\mathbf{I} - c_{10}|^2 dx + \int_{\mathbf{I}_{01}} |\mathbf{I} - c_{01}|^2 dx + \int_{\mathbf{I}_{00}} |\mathbf{I} - c_{00}|^2 dx, \quad (5)$$

where the integration areas are defined by

$$\mathbf{I}_{11} = \operatorname{in}(\mathbf{C}_1) \cap \operatorname{in}(\mathbf{C}_2), \mathbf{I}_{10} = \operatorname{in}(\mathbf{C}_1) \setminus \operatorname{in}(\mathbf{C}_2), \mathbf{I}_{01} = \operatorname{in}(\mathbf{C}_2) \setminus \operatorname{in}(\mathbf{C}_1), \mathbf{I}_{00} = \Omega \setminus \{\operatorname{in}(\mathbf{C}_1) \cup \operatorname{in}(\mathbf{C}_2)\}$$

and $\operatorname{in}(\mathbf{C}_i)$ denotes the region enclosed by \mathbf{C}_i . The constants $c_{11}, c_{10}, c_{01}, c_{00}$ denote the average gray-value of the respective four integration area. The functional (5) is known to be well-suited for MR-brain segmentation (see Angelini et al.¹⁴) as its minimization identifies four areas which ideally should correspond to white matter, gray matter, cerebrospinal fluid, and their complement.

2. METHODS

In this section we present our unified framework for joint segmentation and registration and classify published methods within this framework.

2.1. Unified framework for the joint SEGmentation and regISTRATION (segristration)

An unified framework for non-parametric registration combined with segmentation through active contours is given by the following functional

$$\begin{aligned}
 J(\mathbf{Y}, \mathbf{C}_R, \mathbf{C}_T; \mathbf{R}, \mathbf{T}) = & \beta_1 \cdot J_{SEG}(\hat{\mathbf{C}}; \mathbf{R}) + \beta_2 \cdot J_{SEG}(\mathbf{C}_{T_Y}; \mathbf{T}_Y) \\
 & + \beta_3 \cdot J_{REG}(\mathbf{Y}; \mathbf{R}, \mathbf{T}) + \beta_4 \cdot D_C(\mathbf{Y}, \mathbf{C}_R, \mathbf{C}_T; \mathbf{R}, \mathbf{T}),
 \end{aligned} \tag{6}$$

where $\hat{\mathbf{C}} = \mathbf{C}_R, \mathbf{C}_{T_Y}$. The first two terms are responsible for the segmentation of the reference and deformed template, respectively. They may be supplemented by prior knowledge, like a given segmentation of either one start images. The registration is driven by the third term whereas the last terms provides an explicit link between the two thought after segmentations. It may be seen as a communication term between the registration and segmentation part of the problem.¹⁵ Here, we have used the recently proposed¹⁶ functional

$$D_C(\mathbf{Y}, \mathbf{C}_R, \mathbf{C}_T; \mathbf{R}, \mathbf{T}) = \frac{1}{2} \int_{\Omega} \left(\text{in}(\mathbf{C}_{T_Y}(\mathbf{x})) - \text{in}(\mathbf{C}_R(\mathbf{x})) \right)^2 dx, \tag{7}$$

which has a favorable computation complexity as compared to alternative approaches.

Next we show, how to formulate and classify the published methods for the combination of non-parametric image registration and segmentation through active contours within the framework provided by (6). As it turns out, The main difference between these methods is their incorporation of prior knowledge.

2.2. Classification of segristration methods

The published approaches may be divided into three principal branches:

1. **No initial segmentation:** The aim of this case to find a displacement field for the registration and a segmentation of objects in both images. Actually, a segmentation of the template is computed and then carried over to the reference by the computed displacement field. Moreover, registration and segmentation are interacting sequentially. That is, in each iteration, the segmentation uses feedback from the last registration step and vice versa.
2. **Given segmentation of the template image:** In this case we are looking for a segmentation of the reference and for a registration of the segmented template image. Here, the registration and segmentation phase is carried out simultaneously and a communication term is employed.
3. **Given segmentation of the reference image:** Here the segmentation and registration are in addition driven by the given segmentation of the reference. The energy functional of the segmentation serves as an additional distance measure for the image registration, which may be seen as a segmentation guided image registration.

These three branches are described for example by G. Unal et al.,¹⁷ F. Wang et al.,¹⁵ and J. Liu et al.^{18,?} The energy functionals of these approaches are shown in Table 1.

Note that the minimization objects differ in each of the three cases.

Method	energy functional
No initial segmentation: $\hat{\mathbf{C}} = \mathbf{C}_{\mathbf{T}_Y}, \beta_4 = 0$	$J(\mathbf{Y}, \mathbf{C}_{\mathbf{T}}; \mathbf{R}, \mathbf{T}) = \beta_1 \cdot J_{SEG}(\mathbf{C}_{\mathbf{T}_Y}; \mathbf{R}) + \beta_2 \cdot J_{SEG}(\mathbf{Y}, \mathbf{C}_{\mathbf{T}_Y}; \mathbf{T}_Y)$ $+ \beta_3 \cdot J_{REG}(\mathbf{Y}; \mathbf{R}, \mathbf{T})$
Given $\mathbf{C}_{\mathbf{T}}$: $\hat{\mathbf{C}} = \mathbf{C}_{\mathbf{R}}, \beta_2 = 0$	$J(\mathbf{Y}, \mathbf{C}_{\mathbf{R}}; \mathbf{R}, \mathbf{T}) = \beta_1 \cdot J_{SEG}(\mathbf{C}_{\mathbf{R}}; \mathbf{R})$ $+ \beta_3 \cdot J_{REG}(\mathbf{Y}; \mathbf{R}, \mathbf{T}) + \beta_4 \cdot D_C(\mathbf{Y}, \mathbf{C}_{\mathbf{R}}; \mathbf{R}, \mathbf{T})$
Given $\mathbf{C}_{\mathbf{R}}$: $\beta_1 = \beta_4 = 0$	$J(\mathbf{Y}; \mathbf{R}, \mathbf{T}) = \beta_2 \cdot J_{SEG}(\mathbf{C}_{\mathbf{R}}; \mathbf{T}_Y) + \beta_3 \cdot J_{REG}(\mathbf{Y}; \mathbf{R}, \mathbf{T})$

Table 1. Three principal approaches for non-parametric image registration combined with segmentation through active contours.

3. RESULTS

To demonstrate the performance of the described approaches for real clinical problems, we applied them to the registration of two magnet resonance brain images used for diagnostic and therapy of Alzheimer’s disease. The data used in this article was obtained from the Alzheimers Disease Neuroimaging Initiative (ADNI) database (www.loni.ucla.edu/ADNI). For demonstration purposes, we comment on two-dimensional slices of the three-dimensional brain images.

Figure 1(a) illustrates the reference and Figure 1(b) the template image, respectively. The difference between the reference and the template image is displayed in Figure 1(c). It is apparent that the clinically highly relevant ventricles, as well as the skull have quite different positions in the images.

To have a benchmark segmentation, we computed an automatic segmentation of the reference image based on the outlined variation of the Mumford-Shah approach (4). To start the scheme a clever starting guess is needed. Proper choices are discussed in¹⁹. We initialized the segmentation with two sets of initial curves, which were shifted against each other (see Figure 2 (a)). The result of the plain segmentation of reference image is depicted in Figure 2 (b). Here, we performed already a labeling with respect to white matter, gray matter, and cerebrospinal fluid.

Next, we turn our attention to the registration schemes. In all experiments we selected the parameter $\alpha_1 = 1$, $\alpha_2 = 1$, $\lambda = 0$, $\mu = 1$ (elastic potential, for details see²), $\beta_1 = 0,001$, $\beta_2 = 0,001$, $\beta_3 = 1$, and $\beta_4 = 0,0001$. All tests were stopped after 50 steps of a corresponding fixed-point iteration.

It is always advisable, to invoke a non-parametric registration scheme by an affine linear registration step. The resulting image and the corresponding difference are displayed in Figure 3 (a), (b). Note that the ventricles and the scalp are badly registered.

To obtain a benchmark registration we next registered the two images by a plain non-parametric elastic registration scheme. It is apparent from Figure 4 (a), (b) that the registration results are improved but still the ventricles are not optimally aligned.

Next, we applied the registration scheme without a given segmentation (case 1). The results of both the segmentation and registration are depicted in Figure 5. To obtain the segmentation of the reference image we applied the computed displacement field onto the obtained segmentation of the template. As it turned out, the registration result outperforms the one obtained by the plain registration scheme. In particular the ventricles and the scalp are almost perfectly matched. However, it came as a surprise to us, that the obtained segmentation is not as good as the plain one. Although the ventricle are nicely captured the partition in white and gray matter is not satisfying. We will investigate this shortcoming in our future work.

Next, we discuss the case 2 of our registration framework, that is we supplied an a-priori calculated segmentation of the template image and employed the communication distance measure D_C (7). As indicated by Figure 6, the

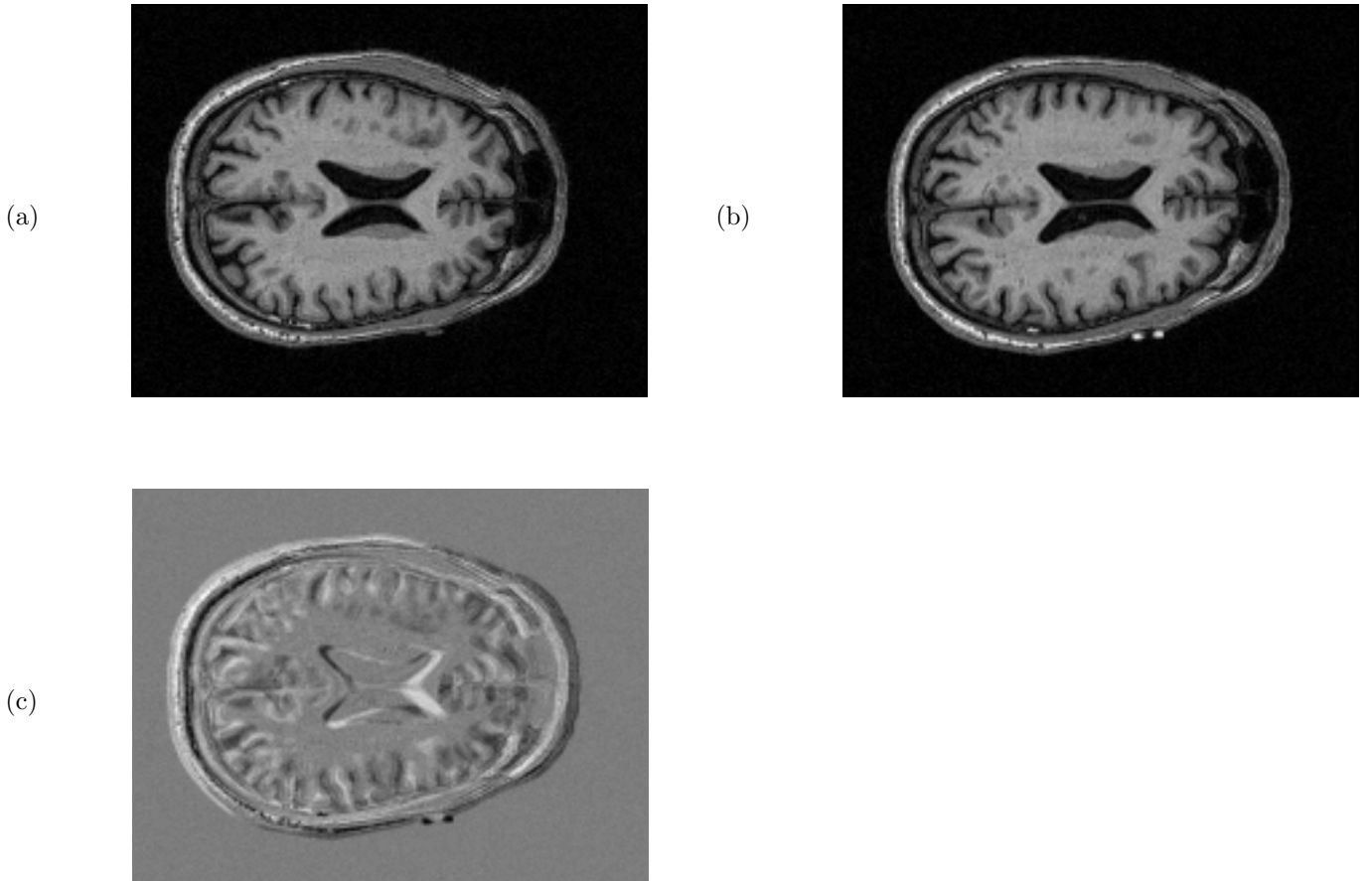


Figure 1. (a) reference image, (b) template image, (c) difference between the reference and template image.

registration result is comparable to the one in Figure 5. This time, however, the segmentation of the final deformed template is much better. Obviously, the scheme benefits from the supplemented segmentation.

Finally, we supplemented a segmentation of the reference image \mathbf{R} (case 3). The results are depicted in Fig. 7. Clearly, the registration result improved a lot as compared to the plain registration. The differences between reference image and the deformed template are in particular small in the area of the ventricles. In this case, the given segmentation acts as a guidance for the registration scheme and is not in the focus on its own.

4. NEW OR BREAKTHROUGH WORK TO BE PRESENTED

We presented for the first time a unified framework for non-parametric registration combined with segmentation through active contours. We have shown, that today's existing methods may be phrased in this framework and that one may now compare these approaches in a fair environment. In particular the elastic registrations scheme combined with the multi-phase variation of the Mumford-Shah segmentation appears to be a very powerful pair.

5. CONCLUSIONS

In the literature one may find various ways to combine image registration and segmentation. It has been the goal of this work to come up with a unified framework for this kind of approach which allows for the incorporation of energy-based segmentation into non-parametric image registration schemes in a systematic and mathematically sound fashion. Our focus has been on the registration part and it has been demonstrated that the outlined methods

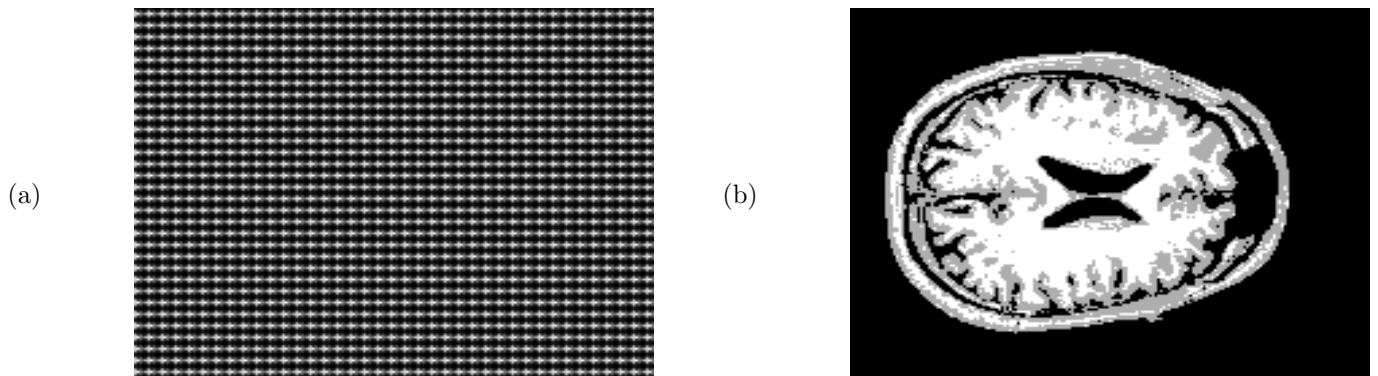


Figure 2. (a) initial contour for the segmentation, (b) result of a multi-phase automatic plain segmentation using the Mumford-Shah functional.

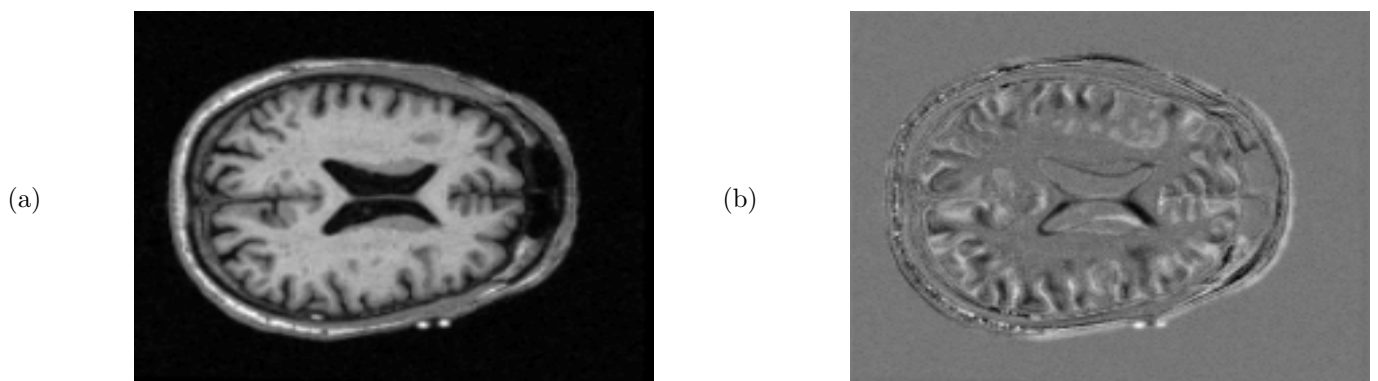


Figure 3. (a) result of an affine linear registration, (b) difference between the reference image and the result.

may improve plain registration results. The approach has been tested on two-dimensional slices of three-dimensional magnet resonance brain images. The evaluation has shown great potential of the proposed framework. In the future we plan to extend of our approach to different segmentation and registration terms. **ACKNOWLEDGEMENTS**

ACKNOWLEDGMENTS

Data collection and sharing for this project was funded by the Alzheimers Disease Neuroimaging Initiative. The authors are thankful to Stewart Young and Fabian Wenzel of the Philips Research Europe - Hamburg for discussions in regard to magnet resonance brain images. We would like to thank Jan Modersitzki of the University of Luebeck, Steffen Renisch and Ingwer Carlsen of the Philips Research Europe - Hamburg for discussions with regard to image registration. This research has been supported by the Philips Research Europe - Hamburg.

REFERENCES

1. K. Ens, H. Schumacher, A. Franz, and B. Fischer, "Improved elastic medical image registration using mutual information," *Proceedings of SPIE 2007, Medical Imaging, San Diego*, 2007.
2. J. Modersitzki, *Numerical methods for image registration*, Oxford University Press, 2003.
3. J. V. Hajnal, D. L. G. Hill, and D. J. Hawkes, *Medical image registration*, CRC Press, Boca Raton, 2001.
4. J. B. A. Maintz and Viergever, "A survey of medical image registration," *Medical Image Analysis* (2(1)), pp. 1–36, 1998.

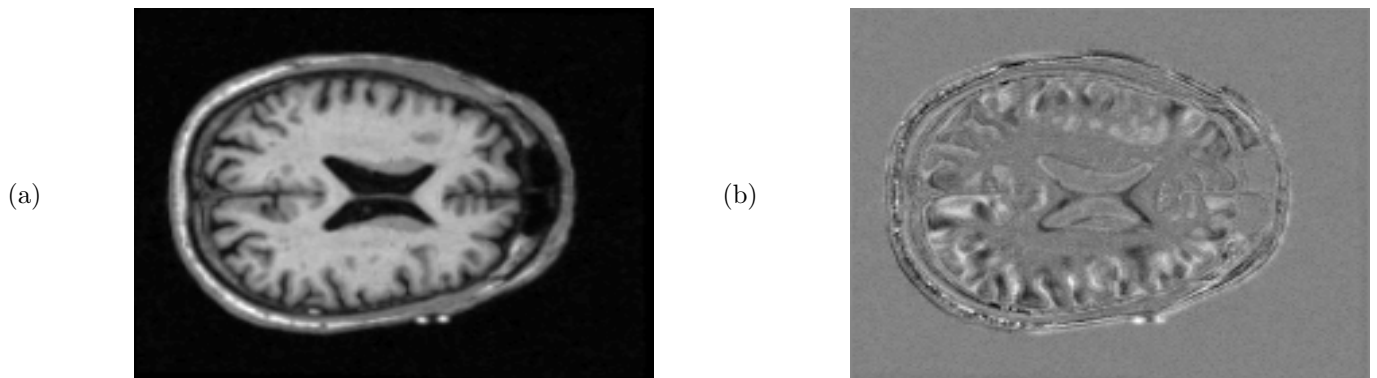


Figure 4. (a) result of a non-parametric elastic registration, (b) difference between the reference image and the result.

5. B. Zitová and J. Flusser, “Image registration methods: A survey,” *Image Vision and Computing* **21**(11), pp. 977–1000, 2003.
6. N. Papenberg, H. Schumacher, S. Heldmann, S. Wirtz, S. Bommersheim, K. Ens, J. Modersitzki, and B. Fischer, “A fast and flexible image registration toolbox - design and implementation of the general approach.,” In *Bildverarbeitung für die Medizin*. Springer, 2007.
7. C. Broit, *Optimal Registration of Deformed Images*. PhD thesis, Computer and Information Science, Uni Pennsylvania, 1981.
8. P. A. Viola and W. M. Wells III, “Alignment by maximization of mutual information,” in *Fifth International Conference on Computer Vision, IEEE*, pp. 16–23, 1995.
9. L. Hoemke, *A multigrid method for elastic image registration with additional structural constraints*. PhD thesis, Institute of Mathematics, University of Duesseldorf, 2006.
10. S. J. Osher and R. P. Fedkiw, *Level Set Methods and Dynamic Implicit Surfaces.*, Springer, 2002.
11. J. A. Sethian, *Level Set Methods and Fast Marching Methods*, 1996.
12. D. Mumford and J. Shah, “Optimal approximation by piecewise smooth functions and associated variational problems,” *Comm. Pure Appl. Math.* **42**, 1989.
13. T. Chan and L. Vese, “An active contour model without edges,” *Scale-Space LNCS* , 1999.
14. E. D. Angelini, T. Song, B. D. Mensh, and A. F. Laine, “Brain mri segmentation with multiphase minimal partitioning: A comparative study,” *International Journal of Biomedical Imaging* **2007**, p. 15, 2007.
15. F. Wang and B. C. Vemuri, “Simultaneous registration and segmentation of anatomical structures from brain MRI,” in *MICCAI*, pp. 17–25, 2005.
16. K. Ens, J. von Berg, S. Kabus, S. Renisch, and B. Fischer, “A new distance measure for the registration,” *Technical Report, Luebeck* , 2008.
17. C. Unal and G. Slabaugh, “Coupled PDEs for non-rigid registration and segmentation,” in *CVPR*, 2005.
18. J. Liu, “Segmentation guided registration for medical images.,” in *SPIE Medical Imaging*, 2005.
19. L. Vese and T. Chan, “A multiphase level set framework for image segmentation using the mumford and shah model,” *International Journal of Computer Vision* **50**(3) , 2002.

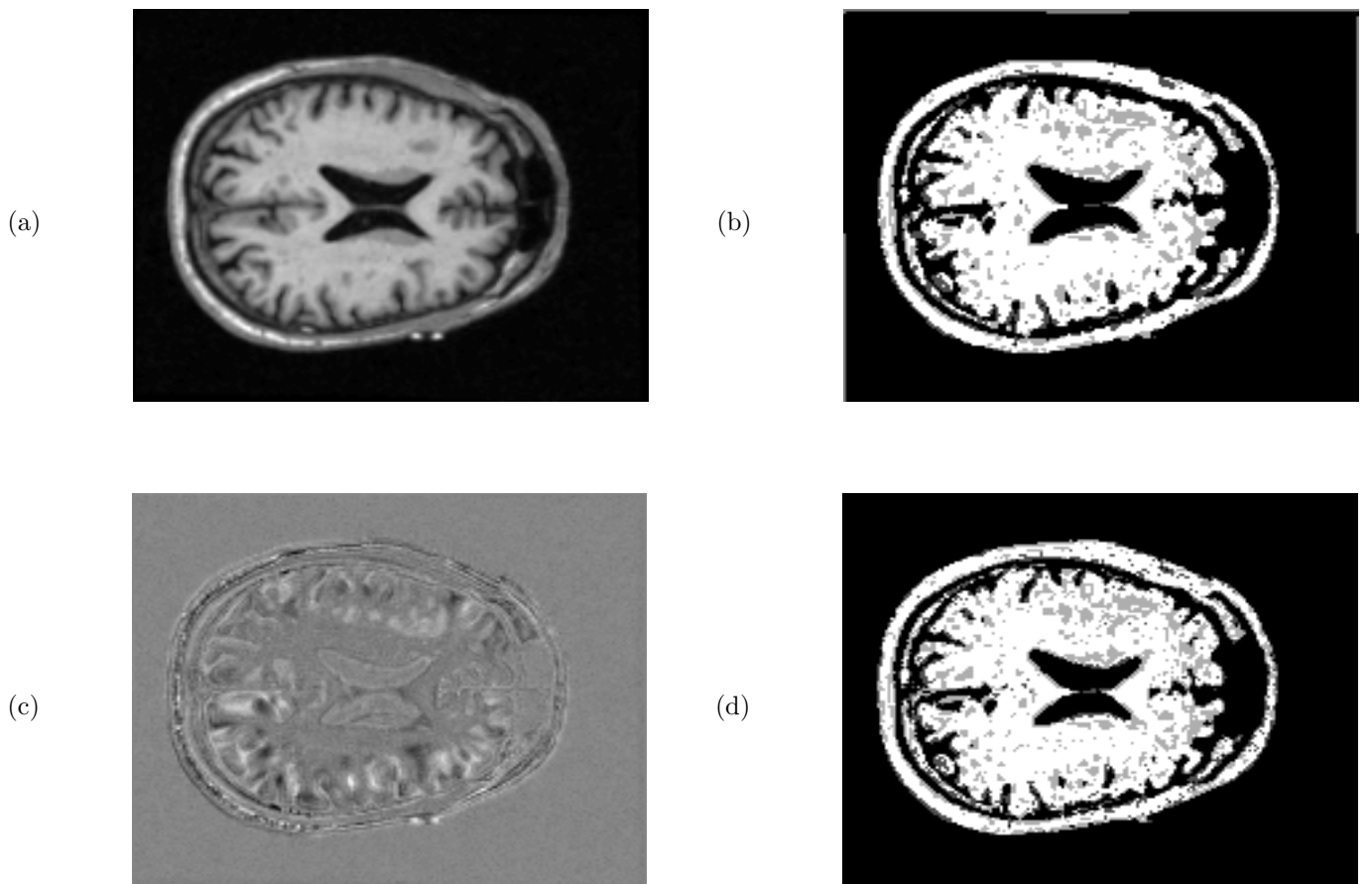


Figure 5. Registration with segmentation without a-priori knowledge : (a) result of registration, (b) segmentation of template , (c) difference between reference image and the result of registration, (d) segmentation of reference.

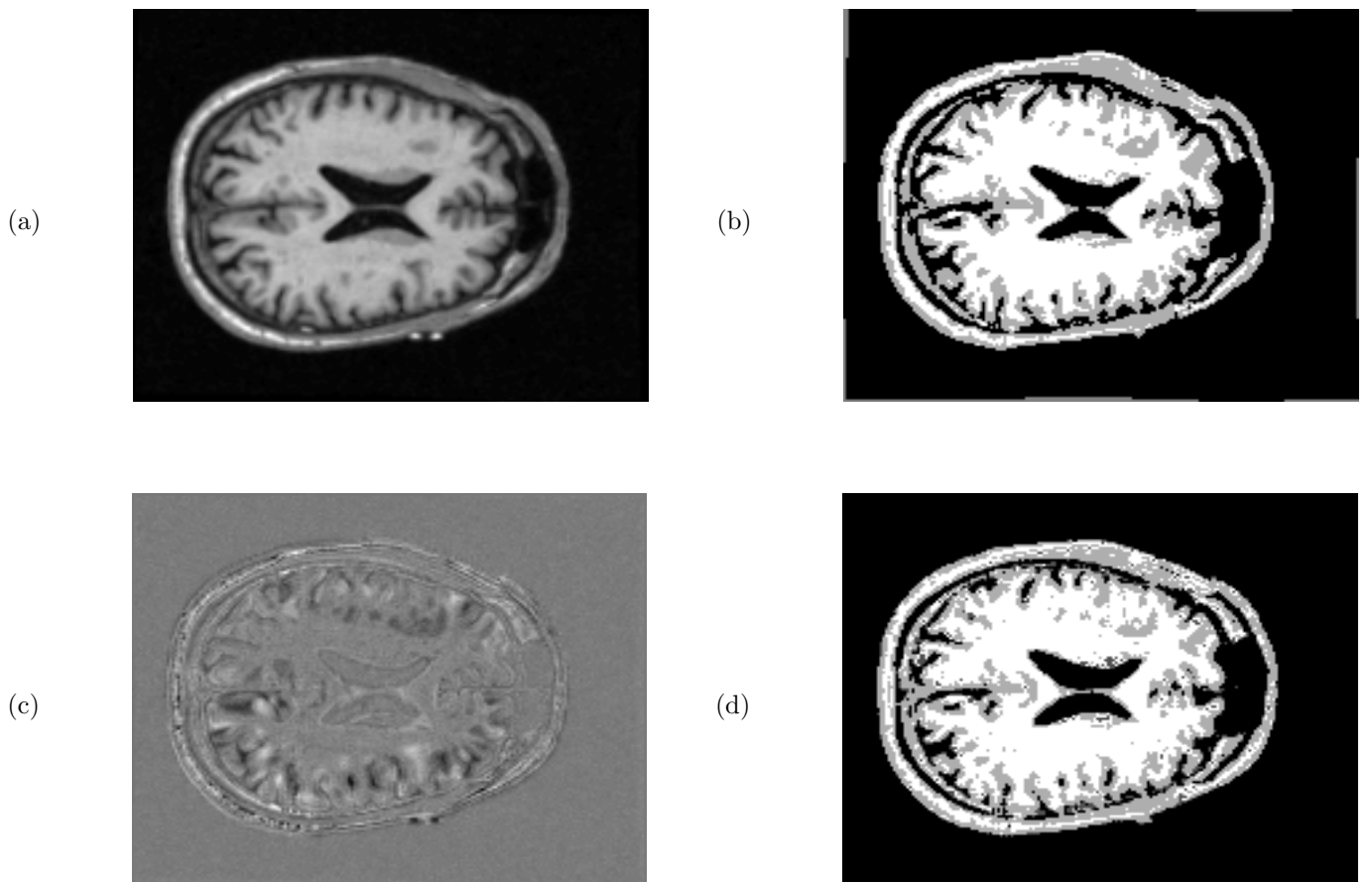


Figure 6. Registration with segmentation with a-priori knowledge about the segmentation of the template image : (a) result of registration, (b) result of registration with segmentation, (c) difference between reference image and the result of registration, (d) segmentation of reference image.

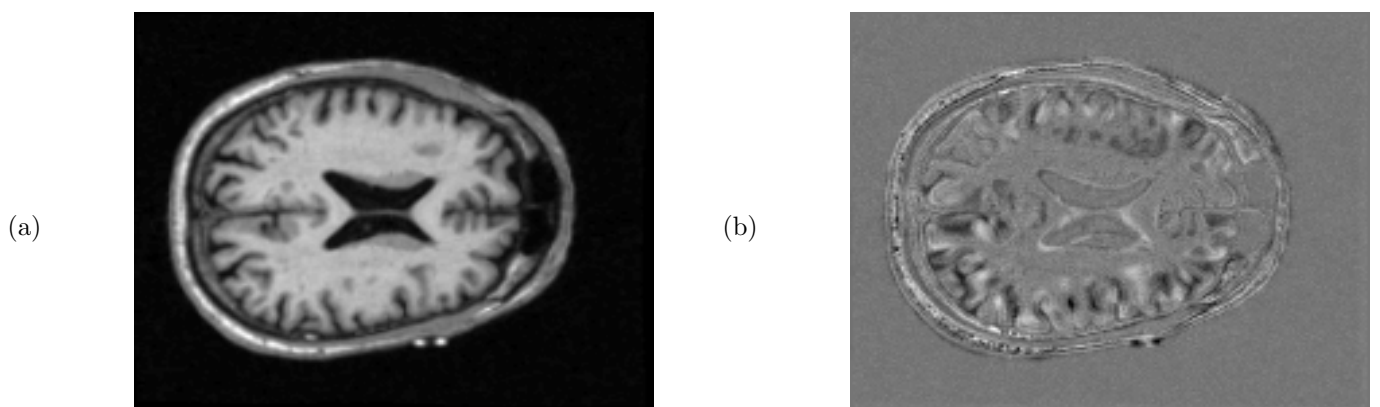


Figure 7. Registration with segmentation with a-priori knowledge about the segmentation of the reference image : (a) result of registration, (b) result of registration with contour/surface of segmentation, (c) difference between reference image and the result of registration.